



## Transition metal atoms encapsulated in adamantane molecules

J.C. Garcia <sup>a</sup>, W.V.M. Machado <sup>b</sup>, L.V.C. Assali <sup>b</sup>, J.F. Justo <sup>a,\*</sup>

<sup>a</sup> Escola Politécnica, Universidade de São Paulo, CP 61548, CEP 05424-970, São Paulo, SP, Brazil

<sup>b</sup> Instituto de Física, Universidade de São Paulo, CP 66318, CEP 05315-970, São Paulo, SP, Brazil

### ARTICLE INFO

Available online 13 July 2011

#### Keywords:

Diamondoids  
Caged molecules  
Nanostructures  
Adamantane

### ABSTRACT

We performed a first principles total energy investigation on the structural, electronic, and magnetic properties of 3d-transition metal-encapsulated adamantane molecules ( $\text{TM}@\text{C}_{10}\text{H}_{16}$ , with  $\text{TM}=\text{Cr}$ ,  $\text{Mn}$ ,  $\text{Fe}$ ,  $\text{Co}$ , and  $\text{Ni}$ ). We find that the C–C interactions are strong enough to maintain the molecular rigidity upon TM incorporation, although outward relaxations and formation energies are large. We built a microscopic model that explains the electronic structure of those molecules.

© 2011 Elsevier B.V. All rights reserved.

### 1. Introduction

Encapsulating atoms, or even small molecules, inside caged nanostructures have attracted considerable attention over the last decade [1,2]. The recent investigations on the properties of transition metal atoms encapsulated in Si, SiC, Ge and Sn caged clusters [3–6] have pointed to potential technological applications ranging from optoelectronic and magnetic devices [4] to medical agents for diagnostics and drug delivery [7,8]. Introducing atoms in the molecular cages may be useful in several aspects; for example it may help to build artificial “super” atoms, quantum systems with tailored electronic properties. Additionally, encapsulating transition metal atoms in those semiconducting molecules has been considered as a way to stabilize them in caged configurations. The resulting stable molecules have been considered in applications as molecular building blocks for nanostructure self-assembly [4].

The Si or Ge small caged molecules are unstable in pristine configurations, since the respective atoms strongly favor the  $\text{sp}^3$ -like bonding over the  $\text{sp}^2$ -like one, and molecules tend to stabilize in more compact forms. Although encapsulating transition metal atoms is a way to energetically favor the cage-like configuration, such procedure is substantially difficult to achieve. However, there are several other caged molecules that are already stable in their pristine configurations, meaning that the only challenge is introducing the transition metal atom in the already stable caged molecules. Although carbon-based molecules are potentially interesting to work as hosts for caged atoms, only fullerenes have been investigated in detail [9]. One of the scarcely explored subjects in the literature concerns encapsulating atoms in hydrocarbons [10].

In the hydrocarbon family, diamondoids are one of the most interesting cases to carry such an investigation. They can be described as molecular diamond, with carbon atoms in a diamond-like microscopic configuration saturated by hydrogen atoms. They have received great attention recently, after successful manipulation out of crude oil [11]. Several applications have been suggested for diamondoids over the years; for example they have been considered for electron emission devices [12], nanosensors, and fundamental building blocks [13–15].

Recent theoretical calculations have studied the interactions of diamondoids with impurities, for example boron and nitrogen atoms in substitutional sites [14,16] and inert and alkali atoms in caged configurations [10]. To our best knowledge there is no investigation in the literature that explores the properties of caged transition metal atoms in those molecules. Here, we used first principles total energy calculations to investigate the properties of embedded 3d-transition metal impurities (Cr, Mn, Fe, Co, and Ni) in adamantane, the smallest diamondoid ( $\text{C}_{10}\text{H}_{16}$ ). We find that the resulting molecules remain stable after the TM inclusion, as a result of the strong carbon–carbon interactions, although large outward relaxation is observed. Additionally, the resulting molecules present interesting magnetic properties, which could be suitable to work as molecular spin valves.

### 2. Methodology

The properties of encapsulated 3d-transition metals in adamantane molecules ( $\text{TM}@\text{C}_{10}\text{H}_{16}$ ) were computed using the Vienna *ab initio* simulation package (VASP) [17]. The electronic exchange correlation potential was described with the generalized gradient approximation of Perdew–Burke–Ernzerhof (PBE) [18] within the spin polarized density functional theory. The electronic wavefunctions were described by a projector augmented wave (PAW) methodology [19] and expanded in a plane-wave basis set, with a

 Presented at the Diamond 2010, 21st European Conference on Diamond, Diamond-Like Materials, Carbon Nanotubes, and Nitrides, Budapest.

\* Corresponding author. Tel.: +55 11 3091 5310; fax: +55 11 3091 6831.

E-mail address: [jjusto@lme.usp.br](mailto:jjusto@lme.usp.br) (J.F. Justo).

kinetic energy cutoff of 400 eV. The system was allowed to relax self-consistently, with no symmetry or spin constrains, with convergence criteria for total energy set to 0.01 meV/unit cell between two self-consistent iterations, and criteria for forces (per atom) set to less than 5 meV/Å.

For each molecule, we also simulated several possible magnetic states, by constraining the molecular magnetization. However, we found that the ground state was associated with the low spin configuration in all cases. The TM atomic characters of the energy levels were identified based on the decomposition of the charge density inside the TM atomic spheres, defined by the PAW method, according to the secondary quantum numbers  $\ell$ .

We considered the TM@C<sub>10</sub>H<sub>16</sub> molecules inside a cubic 15 × 15 × 15 Å<sup>3</sup> simulation cell with periodic boundary conditions. This cell size was large enough to guarantee negligible interactions between the atoms of the molecule in the simulation cell and those in the neighboring cell images (interatomic distances larger than 9.6 Å). Such theoretical framework has been successfully used to investigate several properties of adamantane-related molecules [14,20].

### 3. Results and discussion

Adamantane (C<sub>10</sub>H<sub>16</sub>) is the smallest diamondoid, consisting of a single diamond-like cage that carries two types of carbon atoms, labeled C(1) and C(2). A C(1) is bound to three C(2)'s and one H atom, while a C(2) is bound to two C(1)'s and two H's. C(1)–C(2) interatomic distances are 1.538 Å and angles between two C(1)–C(2) bonds are 109.5°; both results are close to the respective values in crystalline diamond [14]. Since these C–C interatomic distances are very small, one may define adamantane as a compact caged molecule, and it could be anticipated that introducing a transition metal atom in the tetrahedral site of the cage would be energetically costly and cause large outward relaxations.

First of all, our results show that introducing the TM in the tetrahedral interstitial site of adamantane maintains the structural molecular rigidity in the symmetry of the original adamantane molecule. Fig. 1a shows the inclusion energy ( $E_i$ ) for several caged TM atoms. This energy is defined as the difference in energy between a TM@C<sub>10</sub>H<sub>16</sub> configuration and the one with the atomic TM and C<sub>10</sub>H<sub>16</sub> molecule infinitely separated. The figure shows that it costs about 8–10 eV to embed a TM atom inside adamantane. This value should be compared to the inclusion energies of interstitial TM in crystalline diamond, that are in the 12–13 eV range [21]. Here, the inclusion energy of a defect in a crystalline environment is defined as the difference between formation energy of the defect and the TM cohesive energy. Therefore, it is considerably more costly to introduce a TM in diamond than in the adamantane cage.

Fig. 1b shows the interatomic distances between the TM and nearest, TM–C(1), and next-nearest, TM–C(2), carbon neighbors. The TM inclusion in the tetrahedral site caused large outward relaxation respectively of about 16% and 12%. Along the 3d TM series, the TM–C(1) distance maintains approximately constant, while the TM–C(2) one decreases. Additionally, the TM introduction increases the C(1)–C(2) distances by about 13%. These results are fully consistent with the relaxations observed for the respective interstitial TM impurities in diamond [21], as described in the figure. However, since the crystal is more compact than the molecule, it allows smaller outward relaxations. Fig. 1c shows the variations of C–C–C angles ( $\Delta\theta = \theta - \theta_t$ ), with respect to tetrahedral angle ( $\theta_t = 109.47^\circ$ ), as result of TM incorporation in the adamantane cage. Along the 3d TM series, from Cr to Ni, while the C(1)–C(2)–C(1) angles increase with respect to  $\theta_t$ , the C(2)–C(1)–C(2) ones decrease.

The most important properties of caged molecules concern the resulting electronic structure. Fig. 2 shows the 3d-related energy eigenvalues which appear in the adamantane energy gap (the HOMO–LUMO energy region). The transition metal introduces a pair of levels

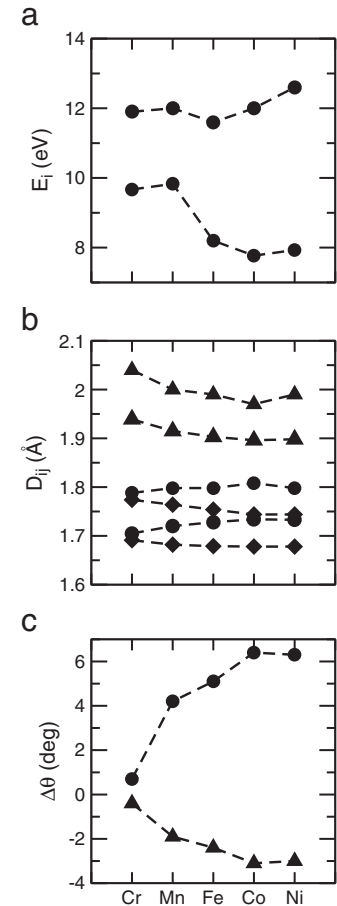


**Fig. 1.** (a) Inclusion energies of a TM on the tetrahedral interstitial site of C<sub>10</sub>H<sub>16</sub> (closed symbols) and diamond (open symbols). (b) Interatomic distances ( $D_{ij}$ ) between the atom  $i$  and its neighboring  $j$  ones in the molecule (closed symbols) and in diamond (open symbols) [21]. The figure shows the TM–C(1) (circle symbols), TM–C(2) (triangle symbols), and C(1)–C(2) (diamond symbols) distances. (c) Variations in the C(1)–C(2)–C(1) (circle symbols) and C(2)–C(1)–C(2) (triangle symbols) angles ( $\Delta\theta$ ) as result of TM introduction in adamantane molecule.

with 3d-t<sub>2</sub> and 3d-e irreducible representations, which came from the splitting of the 3d-level in the tetrahedral ligand molecular field. Along the series, the 3d-related energy eigenvalues move from the top of the gap toward its bottom. These results are fully consistent with trends observed for interstitial TM impurities in several crystalline semiconductors [21–24]. In Cr@C<sub>10</sub>H<sub>16</sub>, the center has an electronic close shell configuration, with spin  $S=0$  (a fully occupied 3d-t<sub>2</sub> level). In going from Cr to Mn, the additional electron is accommodated in the 3d-e levels. Along the series, this 3d-e level accommodated the

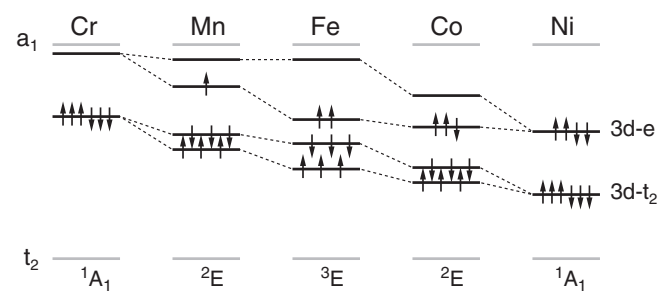


**Fig. 2.** Energy eigenvalues related to the TM-3d states in the HOMO–LUMO energy region for the TM@C<sub>10</sub>H<sub>16</sub> molecules, with TM = Cr, Mn, Fe, Co and Ni. The number of up (down) arrows represents the spin up (down) electronic occupation of the levels. The gray lines are the adamantane-related HOMO and LUMO.

additional electrons, until Ni, which has a close shell configuration with spin  $S=0$  (fully occupied  $3d-t_2$  plus  $3d-e$  levels). The molecules with Mn, Fe, and Co present magnetic properties, with the  $Fe@C_{10}H_{16}$  presenting the highest spin of this series ( $S=1$ ). Since the molecular ligand field is stronger than the on-site exchange interactions, all centers are driven to low spin configurations.

In order to understand the electronic structure of these  $TM@C_{10}H_{16}$  molecules, we built a microscopic model for the interaction between the molecular orbitals of  $C_{10}H_{16}$  and the TM 3d-related ones. When a  $3d^n4s^2$  ion ( $1 \leq n \leq 8$ ) occupies the tetrahedral interstitial site in this molecule, its 4s electrons are transferred to the 3d orbitals, resulting in a  $3d^{n+2}$  configuration. Fig. 3 presents the microscopic model for the  $Cr@C_{10}H_{16}$ , in which Cr assumes a  $3d^6$ , according to the rule described earlier, which is split in  $3d-t_2$  plus  $3d-e$  levels. The major interaction is from a hybridization between the HOMO of adamantane and the  $3d-t_2$  level of atomic Cr. On the other hand, the non-bonding  $3d-e$  level, coming from atomic Cr, remains unaffected and near the LUMO of adamantane. Along the series, from Cr to Ni, electrons are introduced in the  $3d-e$  level, meaning that those orbitals interact very weakly with the surrounding carbon atoms.

Additionally, since the  $3d-t_2$  level remains below the  $3d-e$  one all along the series, consistent with the respective result for interstitial TM in diamond [21], the TM atom interacts more strongly with the C(2) carbon atoms (next-nearest neighbors) than with the C(1) ones (nearest neighbors). This also becomes clear by observing the atomic relaxations in the molecule as result of TM incorporation. As shown in Fig. 1b, interatomic distances TM–C(1) are more affected than TM–C(2) with the TM inclusion, since there is an attractive interaction between the TM and C(2) atoms. This can also be observed in Fig. 1c, in which C(1)–C(2)–C(1) angles increase and C(2)–C(1)–C(2) ones decrease with TM incorporation.

Fig. 4 shows the density probability isosurface of the HOMO and LUMO of adamantane and the respective modifications resulting from Cr inclusion. In adamantane, the HOMO is mostly related to the C(1)–H plus C(1)–C(2) bonds, while the LUMO is related to the C(1)–C(2) bonding, with an anti-bonding character. The Cr inclusion does not affect the LUMO-related level coming from adamantane. However, there is a hybridization between the Cr 3d-related levels and the adamantane HOMO, as discussed in Fig. 3, modifying the HOMO of the original adamantane molecule, which becomes associated with the C(2)–H plus C(1)–C(2) bonds (Fig. 4). The figure also shows the density probability isosurface of the  $3d-t_2$  and  $3d-e$  levels that appear in the energy gap as result of Cr inclusion.

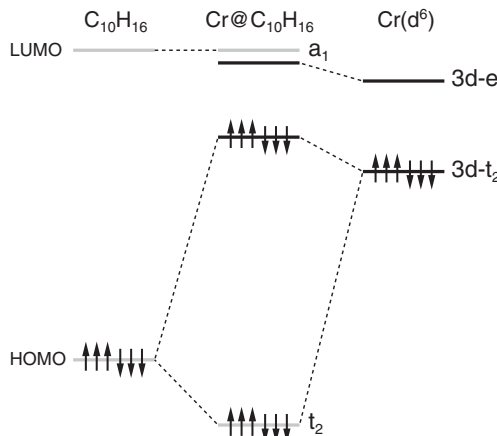


Fig. 3. Microscopic model for the Cr 3d-related energy levels of the  $Cr@C_{10}H_{16}$  molecule as an interaction of adamantane HOMO + LUMO and the atomic Cr  $3d^6$  states in a tetrahedral symmetry.

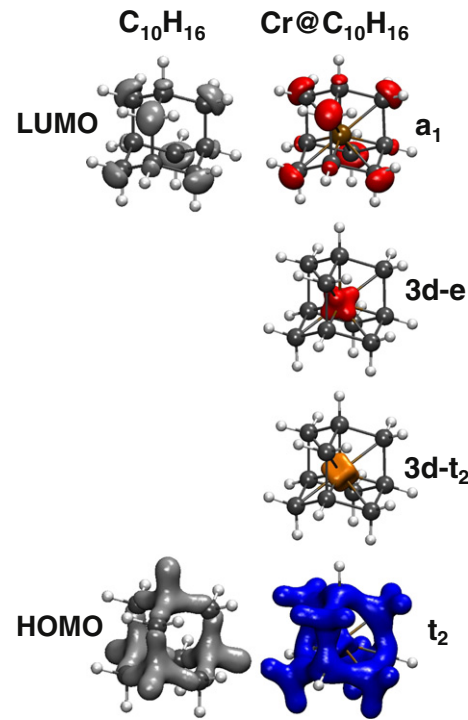


Fig. 4. Density probability isosurfaces of the HOMO and LUMO of  $C_{10}H_{16}$  and gap levels of  $Cr@C_{10}H_{16}$ , according to definition on Fig. 3.

In summary, we have investigated the structural and electronic properties of embedded 3d transition metal atoms in caged adamantane. We find large formation energies and outward relaxations, although the final molecular structure keeps its tetrahedral symmetry. We also built a microscopic model that explains the electronic structure of those molecules.

## Acknowledgments

This work was partially supported by the Brazilian Agencies CNPq and FAPESP.

## References

1. H. Shinohara, Rep. Prog. Phys. 63 (2000) 843.
2. D.A. Britz, A.N. Khlobystov, Chem. Soc. Rev. 35 (2006) 637.
3. V. Kumar, Y. Kawazoe, Appl. Phys. Lett. 83 (2003) 2677.
4. V. Kumar, Y. Kawazoe, Phys. Rev. B 75 (2007) 155425.
5. J. Wang, Q.-M. Ma, R.-P. Xu, Y. Liu, Y.-C. Li, Phys. Lett. A 373 (2009) 2869.
6. B. Song, J. Zhou, Y.L. Yong, P.M. He, J. Phys. Chem. C 114 (2010) 10703.
7. M.V. Yezhelyev, A. Al-Hajj, C. Morris, A.I. Marcus, T. Liu, M. Lewis, C. Cohen, P. Zrazhevskiy, J.W. Simons, A. Rogatko, S. Nie, X. Gao, R.M. O'Regan, Adv. Mater. 19 (2007) 3146.
8. J.C. Garcia, J.F. Justo, W.V.M. Machado, L.V.C. Assali, J. Phys. Chem. A 114 (2010) 11977.
9. A.L. Balch, M.M. Olmstead, Chem. Rev. 98 (1998) 2123.
10. F. Marsusi, K. Mirabbasadeh, J. Phys. Condens. Matter 21 (2009) 215303.
11. J.E. Dahl, S.G. Liu, R.M.K. Carlson, Science 299 (2003) 96.
12. N.D. Drummond, Nat. Nanotechnol. 2 (2007) 462.
13. R.C. Merkle, Nanotechnology 11 (2000) 89.
14. J.C. Garcia, J.F. Justo, W.V.M. Machado, L.V.C. Assali, Phys. Rev. B 80 (2009) 125421.
15. J.C. Garcia, L.V.C. Assali, W.V.M. Machado, J.F. Justo, J. Phys. Condens. Matter 22 (2010) 315303.
16. G.C. McIntosh, M. Yoon, S. Berber, D. Tománek, Phys. Rev. B 70 (2004) 045401.
17. G. Kresse, J. Furthmüller, Phys. Rev. B 54 (1996) 11169.
18. J.P. Perdew, K. Burke, M. Ernzerhof, Phys. Rev. Lett. 77 (1996) 3865.
19. G. Kresse, D. Joubert, Phys. Rev. B 59 (1999) 1758.
20. J.C. Garcia, J.F. Justo, W.V.M. Machado, L.V.C. Assali, Diamond Relat. Mater. 19 (2010) 837.
21. L.V.C. Assali, W.V.M. Machado, J.F. Justo, Physica B 404 (2009) 4515.
22. L.V.C. Assali, J.F. Justo, Phys. Rev. B 58 (1998) 3870.
23. J.F. Justo, L.V.C. Assali, Int. J. Mod. Phys. B 13 (1999) 2387.
24. S. Zhao, L.V.C. Assali, J.F. Justo, G.H. Gilmer, L.C. Kimerling, J. Appl. Phys. 90 (2001) 2744.